

Armando C. Gonzalez,¹ Heidi Multhopp,¹ Robert F. Cook,¹
Brian R. Lawn,¹ and Stephen W. Freiman¹

Fatigue Properties of Ceramics with Natural and Controlled Flaws: A Study on Alumina

REFERENCE: Gonzalez, A. C., Multhopp, H., Cook, R. F., Lawn, B. R., and Freiman, S. W., "Fatigue Properties of Ceramics with Natural and Controlled Flaws: A Study on Alumina," *Methods for Assessing the Structural Reliability of Brittle Materials. ASTM STP 844*, S. W. Freiman and C. M. Hudson, Eds., American Society for Testing and Materials, Philadelphia, 1984, pp. 43-56.

ABSTRACT: A systematic study has been made of the fatigue properties of an as-fired polycrystalline alumina containing either "natural" (sawing damage) or indentation-induced (Vickers) strength-controlling flaws. All fatigue strengths were measured in four-point bending in water. The study is presented in three steps: first, comparative Weibull analyses are made of inert strength data for the two flaw types, both to demonstrate the reduction in scatter that attends the indentation method and to characterize the flaw distributions for the as-sawn surfaces; next, fatigue data are taken on indented surfaces to determine relatively accurate fracture parameters for the alumina and to confirm that constant stressing rate tests can be used as a base for predicting the response in static loading; finally, the results from the two previous, independent steps are combined to generate lifetime responses for the surfaces with natural flaws, and fatigue data taken on such surfaces are used to evaluate these predictions. It is emphasized that residual stresses around the critical flaws (associated either with the preceding contact events responsible for creating the flaws or with extraneous processing, preparation, or service conditions) can play a crucial role in the fracture mechanics. Notwithstanding this complication, the present approach offers a new design philosophy, with the potential for predicting responses relating to flaws generated after, as well as before, any laboratory screening tests.

KEY WORDS: alumina, fatigue, indentation flaw, lifetime prediction, residual stresses, strength testing, structural reliability, brittle materials

In the preceding paper [1] a case was made for using indentation flaws to investigate the fracture properties of candidate materials for structural applications. The indentation method allows for complete control over the forces used

¹Engineer, guest student, graduate student, physicist, and engineer, respectively, Center for Materials Science, National Bureau of Standards, Washington, D.C. 20234.

to generate the critical flaws, provides knowledge of the local stress state of these flaws prior to strength testing, and reduces the scatter in the ensuing failure stresses. Most important, it divides the general strength problem into its two constituent parts, facilitating truly independent determinations of intrinsic material parameters and extrinsic flaw distribution characteristics. This opens the way to a new approach to design, whereby much of the empiricism and statistical data handling associated with conventional strength testing might be avoided.

In this study we demonstrate the approach on a commercial alumina. Alumina was chosen because of its widespread use as a structural ceramic, its availability in large quantities, its relatively simple microstructure, and, above all, its well-documented susceptibility to slow crack growth. This last point is a key one, for it highlights the variability that can bedevil fracture mechanics measurements in ceramics; evaluations of the crack velocity exponent n , using both macroscopic crack specimens [2-16]² and fatigue strength tests [6-8],² lie anywhere between 30 and 90. Part of this variability is no doubt attributable to differences in the source materials. However, the increasing recognition that most techniques in current use for monitoring crack growth are subject to systematic error [9], coupled with the strong influence that any residual stress fields around the critical flaws have on the slopes of fatigue curves [1], can also account for significant discrepancies. The recent comparative study by Pletka and Wiederhorn of double torsion and strength tests on common-source aluminas and other ceramics suggests that such discrepancies could easily exceed a factor of three [6]. There would appear to be a need for greater awareness of the oversimplistic assumptions that are implicit in our present descriptions of crack growth laws, at both the macroscopic and microscopic levels.

The central aim of the present work is to characterize the strength properties of alumina specimens containing "controlled" flaws in order to optimize the amount of testing that must be carried out on similar specimens with "natural" flaws. More specifically, it is intended that crack growth parameters for the alumina should be obtained from dynamic fatigue results on indented surfaces, and flaw distribution parameters from independent inert strength tests on as-prepared surfaces, enabling the two vital elements of the lifetime prediction problem to be treated separately. Predictions made using this approach will be tested against representative fatigue data from the latter, natural surfaces.

Experimental Procedure

Preparation of Specimens with Different Flaw Types

The aluminum oxide used in this study was a roll-compacted, sintered substrate material with 4% additive component (AD96, Coors Porcelain, Colo-

²B. J. Koepke, Honeywell, unpublished work, 1980.

rado), having an average grain size $\approx 10 \mu\text{m}$. It was obtained as plates 1.3 mm thick in its as-fired state and was diamond-sawn into strips 30 mm long and 5 mm wide. Inspection of these strips in the optical microscope revealed chipping damage at the edges. One group of specimens was immediately selected out, at random, and set aside for testing in the as-received state.

The remaining specimens were used for controlled-flaw testing. Each member of this group was indented at a face center with a Vickers diamond pyramid, care being taken to orient the impression diagonals parallel to the specimen edges. For this purpose, a standard load of $P = 5 \text{ N}$ was chosen; this represented a compromise between the requirements that the radial cracks extending from the impression corners should be sufficiently large in comparison with the scale of the impression itself, and yet sufficiently small in comparison with the specimen thickness [10]. All indentations were made in air and were allowed to sit $\approx 1 \text{ h}$ prior to strength testing. Optical and scanning electron microscopical examination of representative examples on surfaces prepolished through $3\text{-}\mu\text{m}$ diamond paste showed that the crack patterns thus produced were not generally of the ideal radial geometry, because of microstructural complications [11], as is evident in the photomicrograph of Fig. 1. The inden-

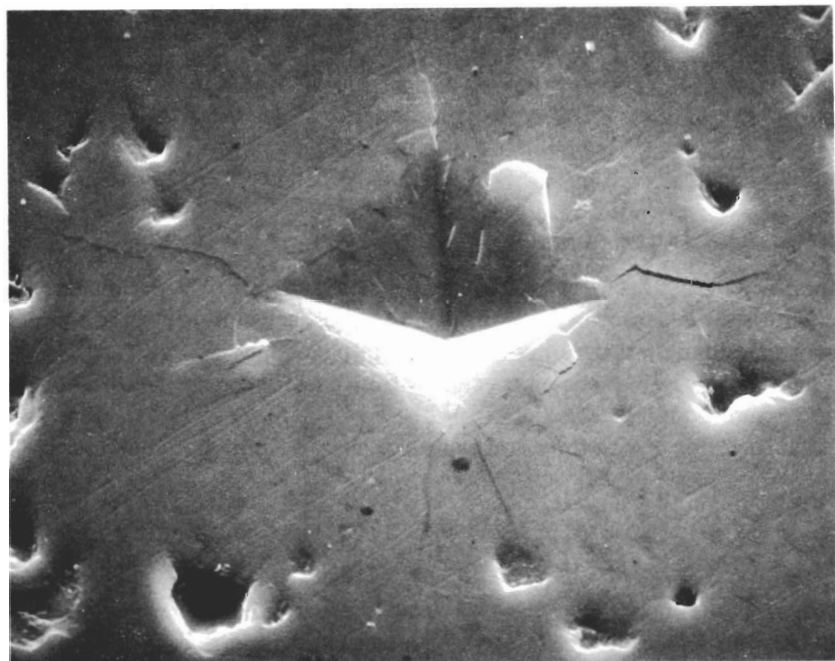


FIG. 1—Scanning electron micrograph of a Vickers indentation flaw in alumina. Note the irregular nature of the radial cracking about the hardness impression. Indentation load $P = 5 \text{ N}$; width of field $150 \mu\text{m}$.

tations were nevertheless sufficiently well formed to allow hardness determinations and, to a lesser extent, crack size measurements to be made.

Strength Testing

The alumina bars prepared as previously described were loaded to failure in four-point flexure, outer span 27 mm and inner span 9 mm, with the surfaces containing the indentation flaws on the tension side. Inert strengths were measured in nitrogen gas or silicone oil, fatigue strengths in water. The inert strength and dynamic fatigue tests were run using a crosshead loading machine, the former at the fastest available rate. Breaking loads were measured by strain-gage and piezoelectric cells [10]. For the static fatigue tests the load was applied pneumatically,³ with a nominal rise time of 8 s and a maximum fluctuation of 1% at hold. Simple beam theory was used to evaluate the stresses from the recorded loads.

All the broken test pieces were examined by optical microscopy to confirm the sources of failure. As expected, those specimens with controlled flaws broke from the indentation sites and those without from the as-sawn edges.

Efforts were also made to run double torsion tests on the alumina, to obtain crack velocity parameters as a check on the strength analysis. However, it was not possible to produce well-behaved cracks in this configuration, presumably because of instabilities in the propagation [6]. Double-cantilever beam specimens were also unsatisfactory, because of the difficulty in locating the crack tips.

Results

Inert Strength Tests

Inert strength tests were run to determine flaw statistical parameters, to check for spurious preexisting stresses in the specimen surfaces, and to obtain appropriate toughness parameters for later fatigue analysis.

The first runs were made on specimens from each of the two groups, that is, as-sawn and indented. The data from these runs, shown in Fig. 2, were analyzed in accordance with the usual two-parameter Weibull probability function

$$F = 1 - \exp \left[- \left(\frac{\sigma_m}{\sigma_0} \right)^m \right] \quad (1)$$

where σ_m is the inert strength and m and σ_0 are adjustable parameters. It is seen that the spread in results is indeed smaller for the surfaces with indentation flaws ($m = 12.9$) than for those with natural flaws ($m = 9.8$). Never-

³A. C. Gonzalez and S. W. Freiman, National Bureau of Standards, unpublished work, 1983.

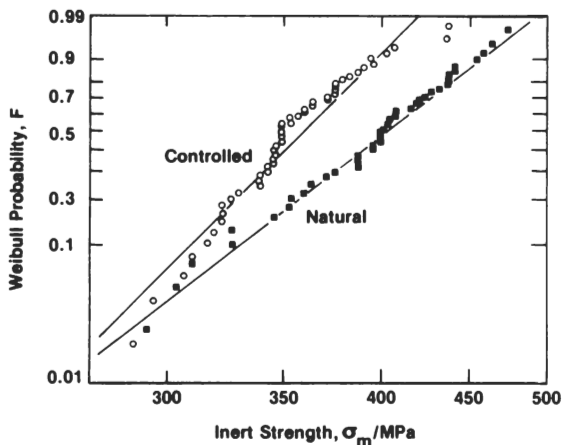


FIG. 2—Weibull plot of inert strengths on alumina surfaces with natural (sawing damage) and controlled (5 N Vickers indentation) flaws.

theless, this spread in the former case is by no means insignificant, consistent with the inherent variability in the crack pattern of Fig. 1.

The next runs were made on indented specimens as a function of the contact load, P . Figure 3 shows the results. The data points represent strengths at $50 \pm 32\%$ Weibull failure probability (equivalent to standard deviation limits for a normal distribution) for at least ten specimens per load, and the straight line is a best fit of slope $-1/3$, in logarithmic coordinates, from which we obtain $\sigma_m P^{1/3} = 590 \pm 47 \text{ MPa N}^{1/3}$ (mean and standard deviation). The constancy of this quantity over the load range covered is an indication of the absence of

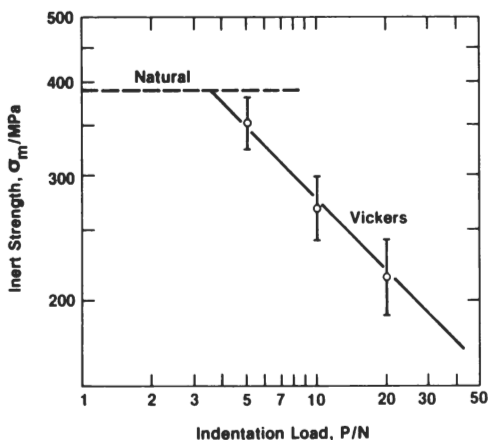


FIG. 3—Inert strength of alumina as a function of Vickers indentation load.

prepresent stresses in the as-fired surfaces [1, 12]. It is noted that the as-sawn strength level in Fig. 3 corresponds to an effective indentation load of 3.3 ± 1.4 N.

Some additional tests were made on prepolished surfaces containing 5-N "dummy" indentations [1, 10]. In these tests, on ten specimens, failure occurred from one of three near-identical contact sites located along the specimen within the inner span, leaving two dummies intact for the determination of the important crack dimensions. Thus, measurements of the set of radial cracks parallel to the tensile direction gave the initial crack dimension of $c_0 = 28 \pm 4 \mu\text{m}$, while those of the perpendicular set gave the critical dimension of $c_m = 33 \pm 5 \mu\text{m}$. The crucial proviso for validity of the fracture mechanics formulation in Ref 1, that is, $c_0 \leq c_m$ is therefore satisfied.

With the underlying basis of the equilibrium fracture description thereby established, we may insert the value of $\sigma_m P^{1/3}$ obtained previously, together with $H = 15.5 \pm 1.0$ GPa measured directly from the hardness impressions and $E = 303$ GPa specified by the manufacturer, into the expression for toughness [1, 13]

$$K_c = \eta \left(\frac{E}{H} \right)^{1/8} (\sigma_m P^{1/3})^{3/4} \quad (2)$$

where $\eta = 0.59$. This gives $K_c = 3.2 \pm 0.2$ MPa $\text{m}^{1/2}$, which may be compared with the value 3.31 ± 0.07 obtained by other workers [14] on similar material using a chevron-notched rod technique.

Dynamic and Static Fatigue of Specimens with Controlled Flaws

Dynamic and static fatigue data were collected on the alumina specimens with standard 5 N indentation flaws, with the purpose of testing the theoretically predicted interrelationships between the two stressing modes.

Figure 4 shows the dynamic fatigue results. The data points are $50 \pm 32\%$ Weibull evaluations of the strengths, σ_f , for at least ten specimens at each of the prescribed stressing rates, $\dot{\sigma}_a$. It is immediately evident that the fatigue strengths are substantially less than the inert strength level, even at the fastest stressing rates. The straight line is a best fit to all individual test results, in accordance with the prediction [1, 15-16]

$$\sigma_f = (\lambda' \dot{\sigma}_a)^{1/(n' + 1)} \quad (3)$$

Bearing in mind the precursor growth stage apparent in the equilibrium failure mechanics referred to in the previous subsection (that is, $c_0 < c_m$), it is important to emphasize that the slope and intercept terms, n' and λ' , relate to *apparent* crack velocity parameters. Appropriate transformation equations for converting these to corresponding *true* parameters obtain from the

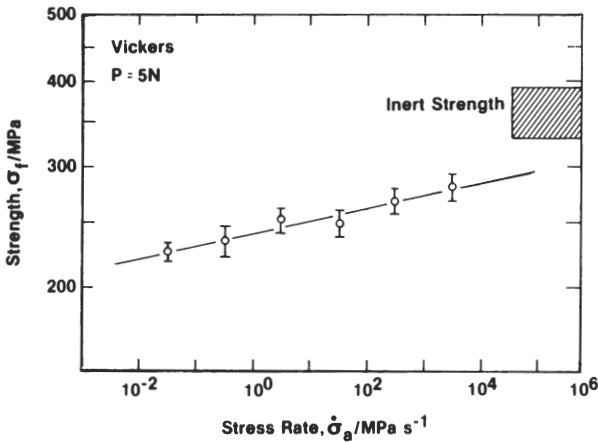


FIG. 4—Dynamic fatigue of alumina in water, for specimens with controlled flaws.

modified stress intensity factors for point flaws with residual contact terms incorporated [1, 16]

$$n' = \frac{3n}{4} + \frac{1}{2} \quad (4a)$$

$$\lambda' = \frac{(2\pi n')^{1/2} \sigma_m^{n'} c_m}{v_0} \quad (4b)$$

where n and v_0 are exponent and coefficient, respectively, in the usual power-law crack velocity relation (Eq 6 in Ref 1). Thus, from the data analysis we obtain $n' = 54.9 \pm 4.9$, which converts, in Eq 4a, to $n = 72.5 \pm 6.5$; also, $\log \lambda' = 133 \pm 12$ (in the units used in Fig. 4), which, in conjunction with the inert strength data from the preceding subsection, yields $\log v_0 = 4.0 \pm 0.5$ (velocity in metres per second).

The corresponding results for the static fatigue tests are shown in Fig. 5. In this case the data are plotted as *median* values of the times to failure, t_f , over ten tests at each of the prescribed holding stresses, σ_A , to accommodate null tests in which the specimens either broke during the loading ramp or survived the two-week cutoff. The straight lines are predictions using the static analogue of Eq 3 [1, 16], that is

$$t_f = \frac{\lambda'}{(n' + 1)\sigma_A^{n'}} \quad (5)$$

where the terms n' and λ' have the same values as previously. As discussed in Ref 1, the procedure is equivalent to inverting the dynamic fatigue curve in ac-

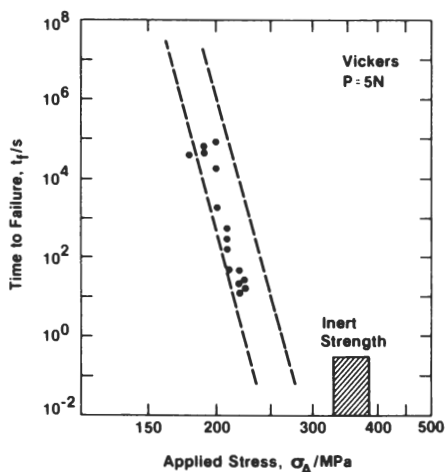


FIG. 5—Static fatigue of alumina in water, for specimens with controlled flaws.

cordance with the relation $t_f = \sigma_f / \dot{\sigma}_a$, identifying σ_f with σ_A , and translating the intercept through $n' + 1$ in logarithmic space. In the spirit of this description we have generated 17 and 83% failure probability limits directly from the corresponding Weibull band for the inert strengths in Fig. 5. The level of agreement between data and predictions in this figure may be taken as a measure of the confidence with which we might use the fatigue equations to analyze the response of less well defined flaws.

Lifetimes of Specimens with Natural Flaws

In this part of the study *a priori* predictions were made of the lifetime characteristics for surfaces with the natural (sawing damage) flaws, using the results of the preceding subsections. Fatigue data were then taken on such surfaces as a check against these predictions.

In adopting this course, we find ourselves confronted immediately by an apparent obstacle, namely, our lack of foreknowledge of the flaw characteristics. If we could assume that the natural flaws were to behave in essentially the same way as the Vickers-induced radial cracks, the procedure would be straightforward enough. Then, one could make use of the "effective" load evaluated at the intersection point of the indentation line, $\sigma_m P^{1/3} = \text{constant}$, with the inert strength level in Fig. 3 to characterize the flaw severity. The appropriate lifetime relation would follow directly from Eq 5, using the same slope parameter, n' , as determined for the indentation flaws but with a load-adjusted intercept parameter [1]

$$\lambda' = \frac{\lambda_p'}{P^{(n' - 2)/3}} \quad (6)$$

where λ'_p is a modified, load-independent term, also to be evaluated from the indentation fatigue data. This prediction is plotted as the solid line in Fig. 6. As in Fig. 5, failure probability limits may be generated directly from the plotted $50 \pm 32\%$ Weibull band for the inert strengths, but these are omitted from the present plot for the sake of clarity.

Unfortunately, the assumption that the strength properties of real materials may be described in terms of ideal point contact flaws does not always hold to good approximation [1]. If the past history of the controlling flaws is such that residual driving forces do indeed persist to stabilize the initial crack growth, but the flaw has essentially *linear* rather than point geometry, the mechanics will reflect the same kind of stress augmentation, but with even greater intensity [17]. Or, if for some reason the residual influence is diminished to an insignificant level, the mechanics will tend closer to those for Griffith flaws (that is, zero residual stress) [18,19]. In either case, the procedure for generating a lifetime prediction remains much the same as before, in that Eq 5 may be retained as the basic starting formula but with the slope term n' in Eq 4a and the intercept term λ' in Eq 4b replaced by appropriate analogues [16]. Expressions for these replacement terms are given in the Appendix; suffice it to say here that evaluations may still be made from the independently obtained dynamic fatigue data on the indented control specimens and inert strength data on the actual specimens with natural flaws. The predictions for these alternative, extreme flaw types are plotted as the broken lines in Fig. 6.

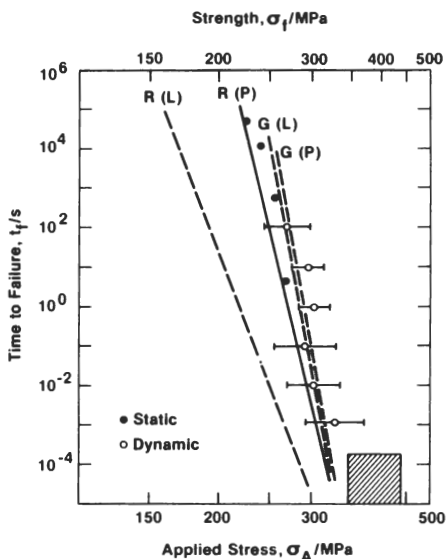


FIG. 6—Lifetime diagram for alumina in water, for surfaces with natural flaws. The lines are predictions based on indentation-calibrated fracture mechanics formulas: R refers to flaws with residual stress, G to conventional Griffith flaws; P and L denote flaws with point and line geometry, respectively. The points are confirmatory static and dynamic fatigue data.

These various predictions for the natural surfaces may be compared with the data points from the confirmatory fatigue tests. Initially, it was intended that all such data should be obtained directly from tests at constant applied stress, but the problems with loading-ramp failures and runouts referred to in connection with Fig. 5, magnified in the case of natural surfaces by the wider spread in flaw severity (that is, lower Weibull modulus), imposed severe limitations on specimen and time economy. Therefore, supplementary data were collected in the constant stressing rate mode, using the inversion and translation operation which interrelates Eqs 3 and 5 to evaluate equivalent lifetimes. A difficulty here, of course, is that this conversion operation is contingent on the quantity $n' + 1$, which we cannot specify *a priori*. In our case, we have obtained a working evaluation by regressing on the pooled dynamic fatigue results, in accordance with Eq 3. Accordingly, the data points in Fig. 6 represent median values for 20 to 40 tests at each static holding stress or $50 \pm 32\%$ probability bounds for 10 to 15 tests at each predetermined dynamic stress rate.

Discussion

We have presented results of a strength study on alumina surfaces with both controlled and natural flaws in the context of lifetime design. Currently, it is widely accepted that the most reliable route to this end is via the exclusive and extensive testing of specimens with the same preparation as that of the structural component, regarding Eqs 3 and 5 as empirical relations to be used in conjunction with statistically determined flaw distributions [20]. We have argued for an alternative philosophy, in which inert strength tests on as-prepared surfaces are retained to determine the flaw distributions, but independent tests are run on indented surfaces to evaluate toughness and crack velocity parameters. The most apparent advantage of this approach is a substantial reduction in the uncertainty in the intrinsic, material component of the strength formulation, so that many fewer specimens should need to be broken to attain a specified tolerance in predicted lifetimes.

The one major obstacle we face in adopting this alternative course is the general inability to predetermine the true nature of the strength-controlling flaw in any prospective structural component. We have seen in Fig. 6 that the presence of residual stresses about the flaw center and the geometrical aspect of this flaw configuration can be decisive factors in lifetime response. In the present tests on as-sawn specimens the results would appear to indicate a relatively minor role for these factors. This is not altogether unreasonable, for, although diamond-sawing is a contact-related process, the basic removal mechanism is one of "lateral-crack" chipping [21], and such chipping modes can greatly relieve the residual contact fields [18]. In principle, the extent of such relief mechanisms may be quantified by comparing strength values before and after a full anneal treatment of the natural surfaces, as has been

done in glass [18,19,22]. With many ceramics, however, annealing is impractical, in which case the prudent designer would presume that residual stress components remain fully active. Indeed, in certain cases, such as with machined surfaces, it might well be advisable to adopt the ultraconservative path and work on the assumption that the flaws also have essentially linear geometry. There is clearly the prospect of overdesign with this approach, which may be unacceptable in applications where the limits of material performance are an absolute necessity. Any decision to design on a less conservative basis, on the other hand, should be backed up with confirmatory fatigue data, such as in Fig. 6. Then, of course, we shall have had to revert, at least in part, to precisely the kind of testing we have sought to supplant in the first place.

With due acknowledgment of the complication just discussed, we may now reinforce our case for the controlled-flaw procedure advocated in this work by emphasizing some of the unique advantages which attend the broad field of indentation fracture mechanics [23-25]. Most important, the approach offers, with its physical insight into the underlying micromechanics of flaw development, the prospect of accommodating changes in the flaw characteristics *subsequent to the laboratory screening tests* within the design specifications. Such changes can be particularly dangerous if they are associated with the spontaneous initiation of *new* flaws, due, for example, to interactions with a hostile mechanical [24,26,27] or chemical [28] service environment. Under these conditions any amount of laboratory testing on as-prepared surfaces would be totally useless if the new flaws were to be dominant. However, provided that the potential service environment is specifiable, indentation fracture mechanics provides us with the facility for estimating an equivalent indentation load for any such flaw; in a particle erosion field, for instance, the load is readily calculable in terms of the incident particle energy and quasi-static component hardness [27]. The problem is thereby reduced to the level of the prepresent natural flaw, whence Eq 6 may be invoked, as before, to obtain a lifetime prediction from Eq 5.

Another distinctive advantage of the indentation flaw method is that one can check routinely for spurious stresses in the as-prepared surfaces. The presence of such stresses becomes manifest as a breakdown in the fracture mechanics formalism used earlier in this work, most conveniently in the inert strength response as a departure from the load independence of the quantity $\sigma_m P^{1/3}$ [1]. (Indeed, *quantitative* information on surface compression stresses has been determined in this manner for tempered glasses [29,30]). Insofar as the lifetime predictions in Fig. 6 are concerned, the effect of a superposed spurious stress may be regarded in terms of an appropriate displacement of all plotted points, in absolute terms, along the horizontal axis, thereby introducing a greater or lesser degree of curvature in the logarithmic representation [15]. This curvature may pass unnoticed in tests on natural surfaces, depending on the scatter in data and range in failure times covered, yet lead to significant discrepancies in long-term extrapolations.

Acknowledgments

The authors thank Dan Briggs of Coors Porcelain Co. for supplying the alumina plates used in this study. Funding was provided by the U.S. Office of Naval Research (Metallurgy and Ceramics Program).

APPENDIX

In interpreting the fatigue results for specimens with natural flaws it was indicated that Eqs 3 and 5 may be retained as the basis for analysis, provided that the quantities n' in Eq 4a and λ' in Eq 4b for point flaws with residual stresses are suitably replaced to match the specific flaw characteristics. Reference is made to the paper by Fuller et al [16] for details.

One of the distinctions we shall be required to make in effecting these conversions is that between geometrical factors for the point and line configurations. The relationship between inert strength, σ_m , and critical crack size, c_m , for the standard point indentations

$$\sigma_m = \frac{3K_c}{4\Psi_p c_m^{1/2}} \quad (7)$$

provides us with the means for doing this: here Ψ_p is a dimensionless factor to be evaluated from the experimental data. An equivalent evaluation for line flaws may then be made purely on theoretical grounds, using an appropriate "modification" relation [31]

$$\Psi_l = \frac{\pi}{2} \Psi_p \quad (8)$$

Consider now the case of linear flaws with fully persistent residual stresses. The replacement quantities in the fatigue equations are

$$n'' = \frac{n}{2} + 1 \quad (9a)$$

$$\lambda'' = \frac{(4\pi n'')^{1/2} \sigma_m'' c_m}{\nu_0} \quad (9b)$$

where it is understood that σ_m and c_m now pertain to measurements on the natural surfaces. Since crack sizes are not readily measured for failures from natural flaws, it is convenient to eliminate c_m from Eq 9b using the line-flaw analogue of Eq 7

$$\sigma_m = \frac{K_c}{2\Psi_l c_m^{1/2}} \quad (10)$$

Thus, given the calibrated values of Ψ_l and K_c from the standard indentation tests, we are left with the natural inert strength as the controlling variable in Eq 9b. Equation 9 may then be coupled with its indentation-flaw counterpart, Eq 3 in the text, to eliminate n and ν_0 , thus completing the conversion operation.

For flaws with zero residual stress, conventional theory applies. The replacement quantities are

$$n_0 = n \quad (11a)$$

$$\lambda_0 = \left[\frac{2}{(n-2)} \right] \frac{\sigma_0'' c_0'}{\nu_0} \quad (11b)$$

where σ_0' is the inert strength conjugate to the initial flaw size c_0' . In this case the apparent and true crack velocity exponents are identical. The crack size may be eliminated through the familiar inert strength relation

$$\sigma_0' = \frac{K_c}{\Psi c_0'^{1/2}} \quad (12)$$

where Ψ identifies with the geometrical factor for point or line flaws, as appropriate. Thereafter, the procedure is the same as that outlined in the previous sample.

References

- [1] Cook, R. F. and Lawn, B. R., in this publication, pp. 22-42.
- [2] Freiman, S. W., McKinney, K. R., and Smith, H. L., in *Fracture Mechanics of Ceramics*, Vol. 2, R. C. Bradt, D. P. H. Hasselman, and F. F. Lange, Eds., Plenum, New York, 1974, pp. 659-676.
- [3] Evans, A. G., Linzer, M., and Russell, L. R., *Materials Science and Engineering*, Vol. 15, 1974, pp. 253-261.
- [4] Bansal, G. K. and Duckworth, W. H., *Journal of Materials Science*, Vol. 13, 1978, pp. 215-216.
- [5] Ferber, M. K. and Brown, S. D., *Journal of American Ceramic Society*, Vol. 63, 1980, pp. 424-429.
- [6] Pletka, B. J. and Wiederhorn, S. M., *Journal of Materials Science*, Vol. 17, 1982, pp. 1247-1268.
- [7] Rockar, E. M. and Pletka, B. J., in *Fracture Mechanics of Ceramics*, Vol. 4, R. C. Bradt, D. P. H. Hasselman, and F. F. Lange, Eds., Plenum, New York, 1978, pp. 725-735.
- [8] Ritter, J. E. and Humenik, J. N., *Journal of Materials Science*, Vol. 14, 1979, pp. 626-632.
- [9] Freiman, S. W., in *Fracture Mechanics of Ceramics*, Vol. 6, R. C. Bradt, A. G. Evans, D. P. H. Hasselman, and F. F. Lange, Eds., Plenum, New York, 1983, pp. 27-45.
- [10] Cook, R. F., Lawn, B. R., and Anstis, G. R., *Journal of Materials Science*, Vol. 17, 1982, pp. 1108-1116.
- [11] Anstis, G. R., Chantikul, P., Marshall, D. B., and Lawn, B. R., *Journal of the American Ceramic Society*, Vol. 64, 1981, pp. 534-538.
- [12] Marshall, D. B. and Lawn, B. R., *Journal of Materials Science*, Vol. 14, 1979, pp. 2001-2012.
- [13] Chantikul, P., Anstis, G. R., Lawn, B. R., and Marshall, D. B., *Journal of the American Ceramic Society*, Vol. 64, 1981, pp. 539-543.
- [14] Barker, L. M., in *Fracture Mechanics of Ceramics*, Vol. 3, R. C. Bradt, D. P. H. Hasselman, and F. F. Lange, Eds., Plenum, New York, 1978, pp. 483-494.
- [15] Lawn, B. R., Marshall, D. B., Anstis, G. R., and Dabbs, T. P., *Journal of Materials Science*, Vol. 16, 1981, pp. 2846-2854.
- [16] Fuller, E. R., Lawn, B. R., and Cook, R. F., *Journal of the American Ceramic Society*, Vol. 66, 1983, pp. 314-321.
- [17] Symonds, B. L., Cook, R. F., and Lawn, B. R., *Journal of Materials Science*, Vol. 18, 1983, pp. 1306-1314.
- [18] Marshall, D. B. and Lawn, B. R., *Journal of the American Ceramic Society*, Vol. 63, 1980, pp. 532-536.

- [19] Chantikul, P., Lawn, B. R., and Marshall, D. B., *Journal of the American Ceramic Society*, Vol. 64, 1981, pp. 322-325.
- [20] Ritter, J. E., in *Fracture Mechanics of Ceramics*, Vol. 5, R. C. Bradt, A. G. Evans, D. P. H. Hasselman, and F. F. Lange, Eds., Plenum, New York, 1982, pp. 227-251.
- [21] Marshall, D. B., Lawn, B. R., and Evans, A. G., *Journal of the American Ceramic Society*, Vol. 65, 1982, pp. 561-566.
- [22] Marshall, D. B. and Lawn, B. R., *Journal of the American Ceramic Society*, Vol. 64, 1981, pp. C6-C7.
- [23] Lawn, B. R. and Wilshaw, T. R., *Journal of Materials Science*, Vol. 10, 1975, pp. 1049-1081.
- [24] Lawn, B. R., in *Fracture Mechanics of Ceramics*, Vol. 3, R. C. Bradt, D. P. H. Hasselman, and F. F. Lange, Eds., Plenum, New York, 1978, pp. 205-229.
- [25] Lawn, B. R., in *Fracture Mechanics of Ceramics*, Vol. 5, R. C. Bradt, A. G. Evans, D. P. H. Hasselman, and F. F. Lange, Eds., Plenum, New York, 1983, pp. 1-25.
- [26] Hockey, B. J., Wiederhorn, S. M. and Johnson, H., in *Fracture Mechanics of Ceramics*, Vol. 3, R. C. Bradt, D. P. H. Hasselman, and F. F. Lange, Eds., Plenum, New York, 1978, pp. 379-402.
- [27] Wiederhorn, S. M. and Lawn, B. R., *Journal of the American Ceramic Society*, Vol. 62, 1979, pp. 66-70.
- [28] Dabbs, T. P., Fairbanks, C. J., and Lawn, B. R., in this publication, pp. 142-153.
- [29] Marshall, D. B. and Lawn, B. R., *Journal of the American Ceramic Society*, Vol. 61, 1978, pp. 21-27.
- [30] Chantikul, P., Marshall, D. B., Lawn, B. R., and Drexhage, M. G., *Journal of the American Ceramic Society*, Vol. 62, 1979, pp. 551-555.
- [31] Lawn, B. R. and Wilshaw, T. R., *Fracture of Brittle Solids*, Cambridge University Press, London, 1975, Chapter 3.